Supporting Information

Cobalt Single-Atoms Anchored on Porphyrinic Triazine-based Frameworks as Bifunctional Electrocatalysts for Oxygen Reduction and Hydrogen Evolution Reactions

Jun-Dong Yi,[a] Rui Xu,[a,b] Guo-Liang Chai,[a] Teng Zhang,[a] Ketao Zang,[c] Bing Nan,[d] Hua Lin,[a] Yu-Lin Liang,[d] Jiangquan Lv,[a,b] Jun Luo,[c] Rui Si,[d] Yuan-Biao Huang*[a] and Rong Cao*[a,b]

[a] State Key Laboratory of Structural Chemistry, Fujian Institute of Research on the Structure of Matter, Chinese Academy of Sciences, 155 Yangqiao Road West, Fuzhou 350002, P.R.China.

[b] University of the Chinese Academy of Sciences, Beijing 100049, China.

[c] Center for Electron Microscopy, Institute for New Energy Materials and Low-Carbon Technologies, School of Materials, Tianjin University of Technology, Tianjin 300384, China.

[d] Shanghai Synchrotron Radiation Facility, Shanghai Institute of Applied Physics, Chinese Academy of Sciences, Shanghai 201204, China.

E-mail: ybhuang@fjirsm.ac.cn (Y.-B. Huang); rcao@fjirsm.ac.cn (R. Cao)

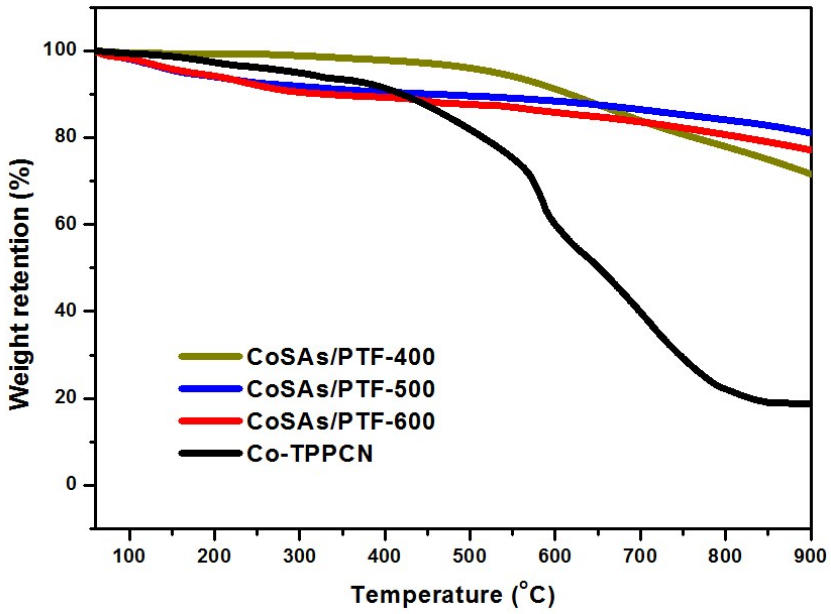

Figure S1. TGA curves of CoSAs/PTF-400, 500, 600 and Co-TPPCN.

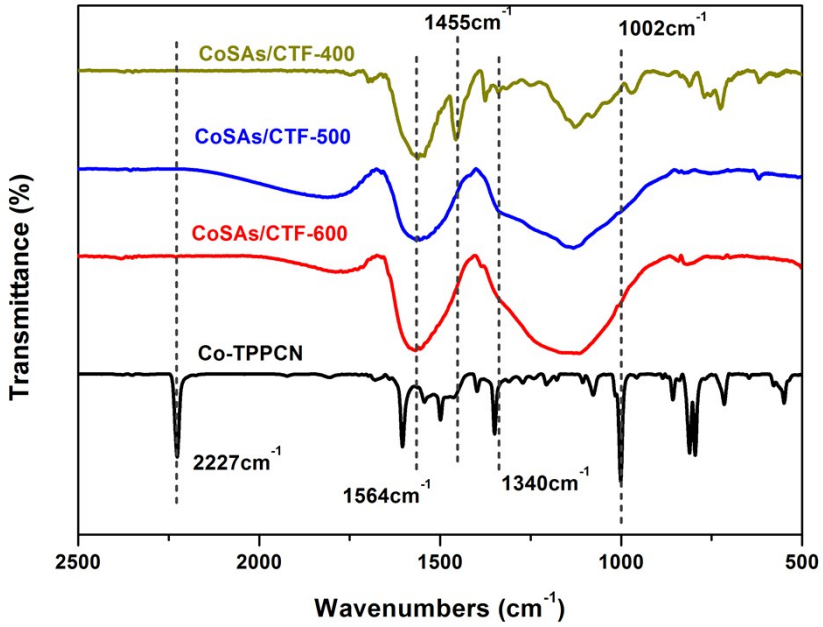

Figure S2. FT-IR spectra of the Co-TPPCN and CoSAs/PTF-*x* (*x* = 400, 500, 600 °C). The characteristic peaks of the Co-N (~1002 cm^{-1}), the stretching vibration of C=N (~1340 cm^{-1}), aromatic ring (~1455 cm^{-1}), the triazine ring (1564 cm^{-1}) and carbonitrile stretching band (2227 cm^{-1}) are marked with dashed line.

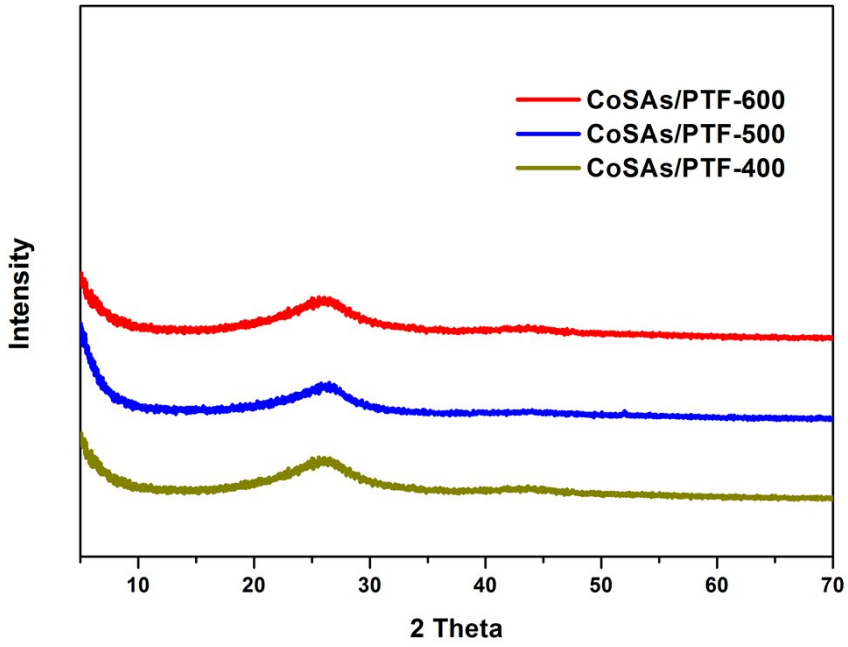

Figure S3. PXRD patterns of CoSAs/PTF-400, 500, 600.

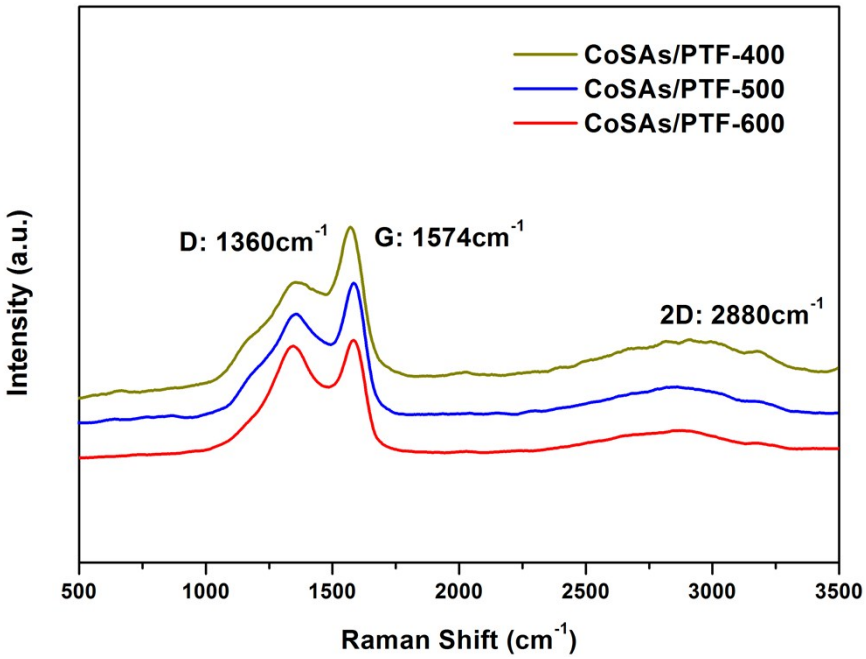

Figure S4. Raman spectra of CoSAs/PTF-400, 500, 600.

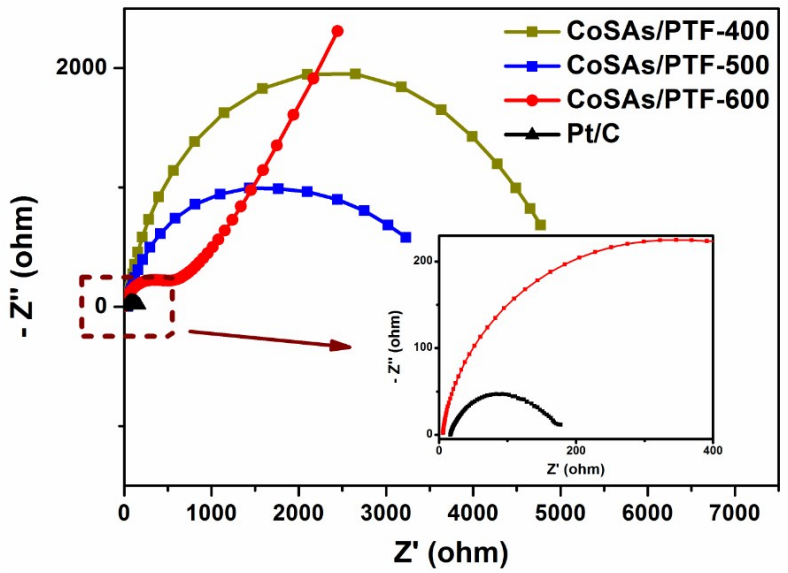

Figure S5. Nyquist plots of different samples over the frequency range from 100 kHz to 10 mHz by applying AC voltage with 5 mV amplitude.

Table S1 R_{ct} values of CoSAs/PTF-400, 500, 600.

Sample	R_{ct} (ohm)
CoSAs/PTF-400	2101
CoSAs/PTF-500	1283
CoSAs/PTF-600	204
Pt/C	75

Table S2 Porous characteristics of CoSAs/PTF-400, 500, 600.

Sample	$S_{langmuir}$ (m^2/g)	S_{BET} (m^2/g)	Tatol Pore Volume (cm^3/g)	Average Pore Size (nm)
CoSAs/PTF-400	1017	668	0.58	3.5
CoSAs/PTF-500	1132	741	0.61	3.3
CoSAs/PTF-600	863	562	0.55	4.0

Table S3. The ICP results of CoSAs/PTF-400, 500, 600.

Sample	Content of Co (wt%)
Monomer-Co	6.89
CoSAs/PTF-400	5.15
CoSAs/PTF-500	2.74
CoSAs/PTF-600	0.85

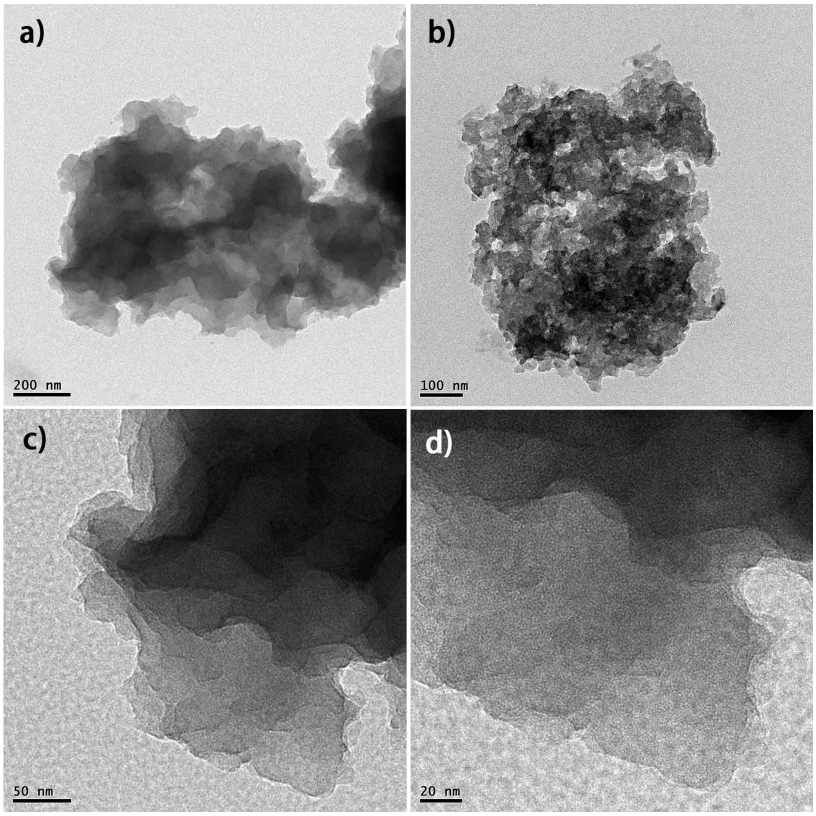

Figure S6. Four representative TEM images of CoSAs/CTF-400 at different areas.

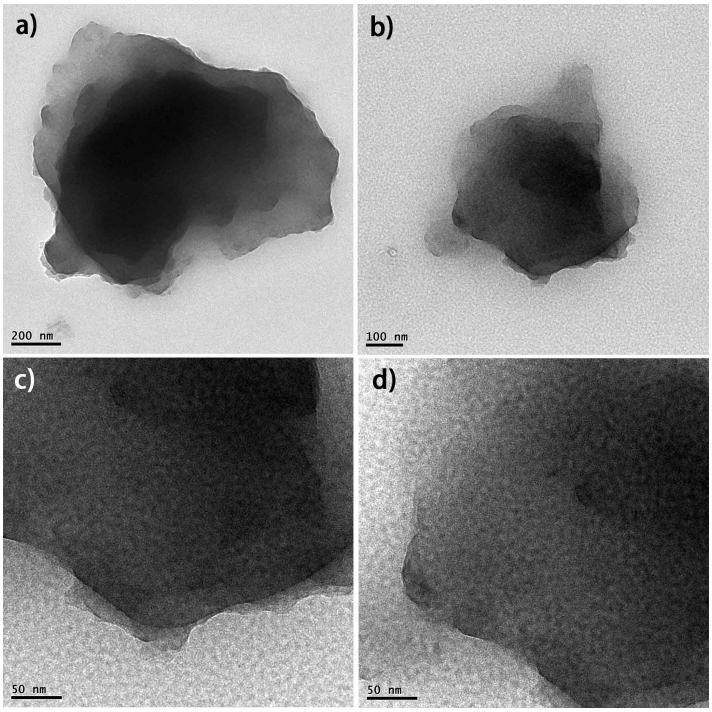

Figure S7. Four representative TEM images of CoSAs/CTF-500 at different areas.

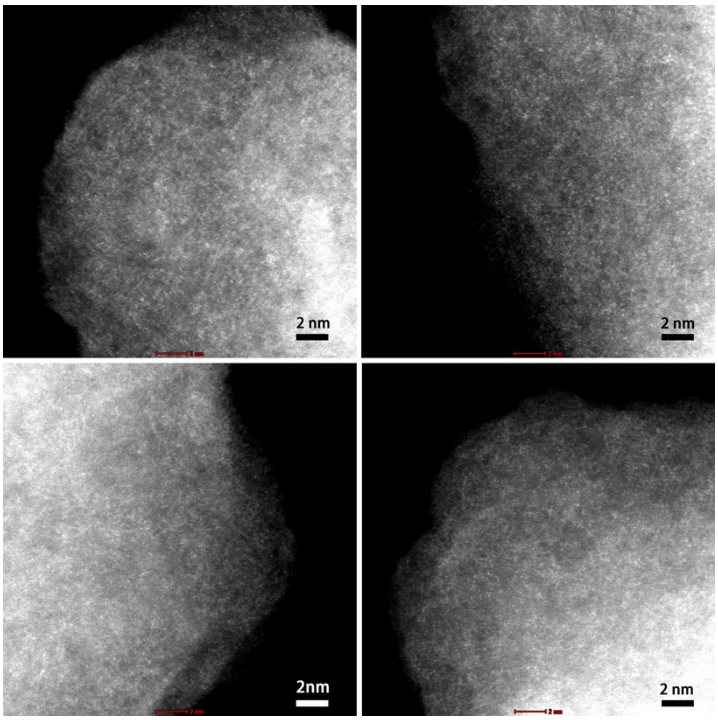

Figure S8. HAADF-STEM images of Co SAs at different areas for the sample CoSAs/CTF-600.

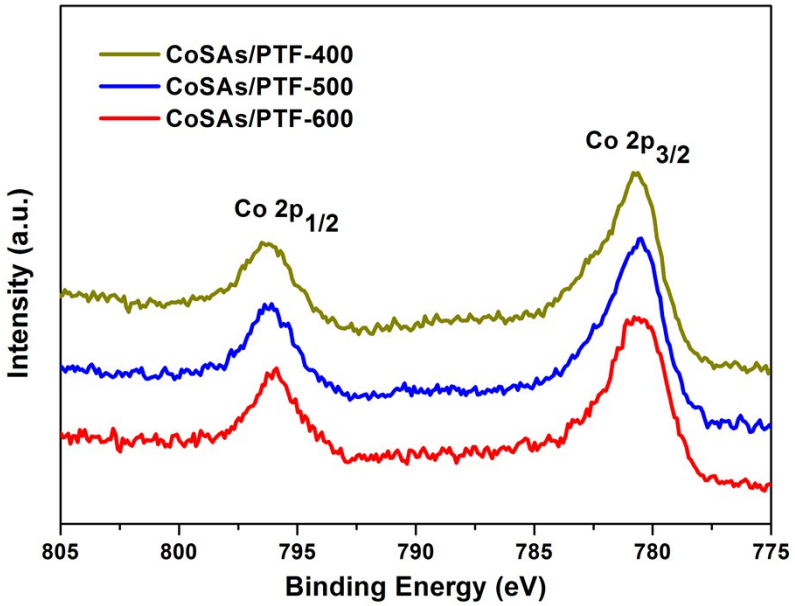

Figure S9. XPS spectra of XPS spectra of the Co 2p region of CoSAs/PTF-400, 500, 600.

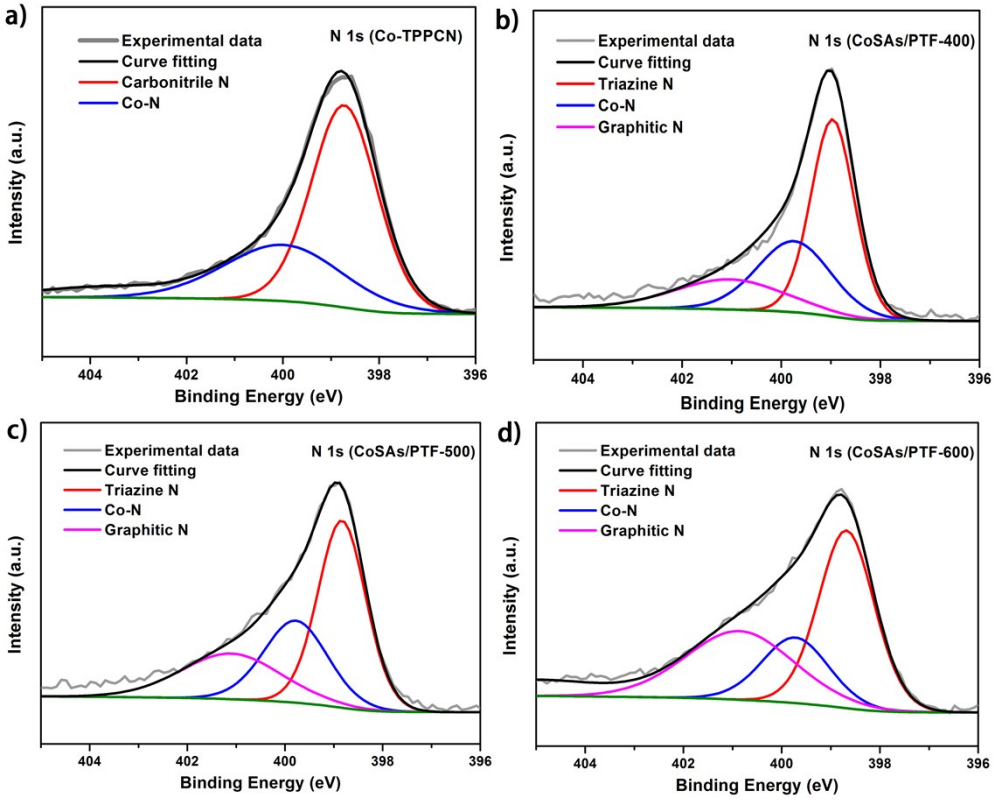

Figure S10. XPS spectra of the N 1s region of a) Co-TPPCN, b) CoSAs/PTF-400, c) CoSAs/PTF-500, d) CoSAs/PTF-600.

Table S4. The content of different types of nitrogen in CoSAs/PTFs based on XPS.

Sample	Triazine N (%)	Graphitic N (%)	Co-N (%)
CoSAs/PTF-400	49.9	19.4	30.7
CoSAs/PTF-500	47.7	24.3	28.0
CoSAs/PTF-600	45.5	34.2	20.3

Table S5 EXAFS data fitting results of Samples.

Sample	Path	CN	*R*(Å)	σ^2(10^{-3} Å^2)	R factor
Co foil	Co-Co	12	2.49±0.01	6.1±0.3	0.0017
CoSAs/PTF-400	Co-N	4.2±0.7	1.90±0.01	8.8±2.1	0.0065
CoSAs/PTF-500	Co-N	3.9±0.7	1.90±0.02	7.1±2.2	0.0097
CoSAs/PTF-600	Co-N	3.9±0.6	1.89±0.01	6.8±1.9	0.0077
Co-TPPCN	Co-N	4.0±0.8	1.96±0.02	7.4±2.2	0.0101

CN, coordination number; R, distance between absorber and backscatter atoms; σ^2, Debye-Waller factor (a measure of thermal and static disorder in absorber-scatterer distances); R factor is used to value the goodness of the fitting.

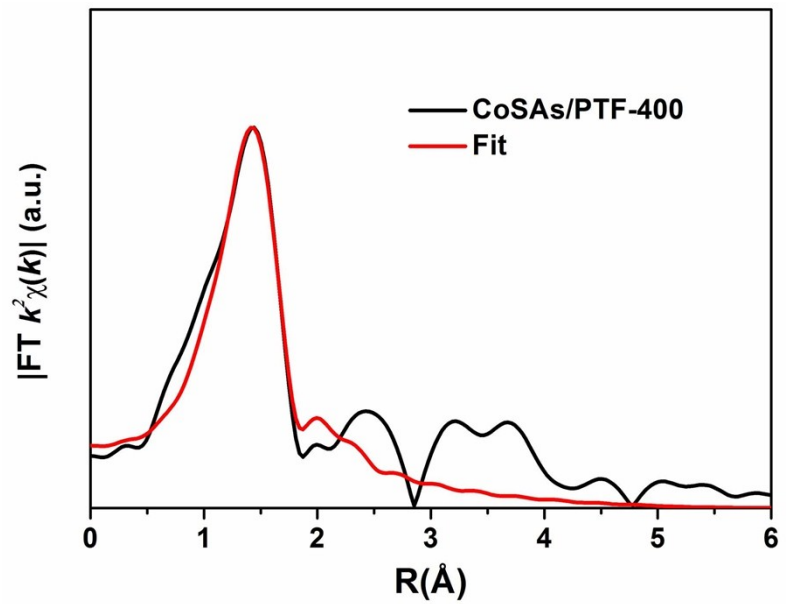

Figre S11. EXAFS fitting curves of CoSAs/PTF-400.

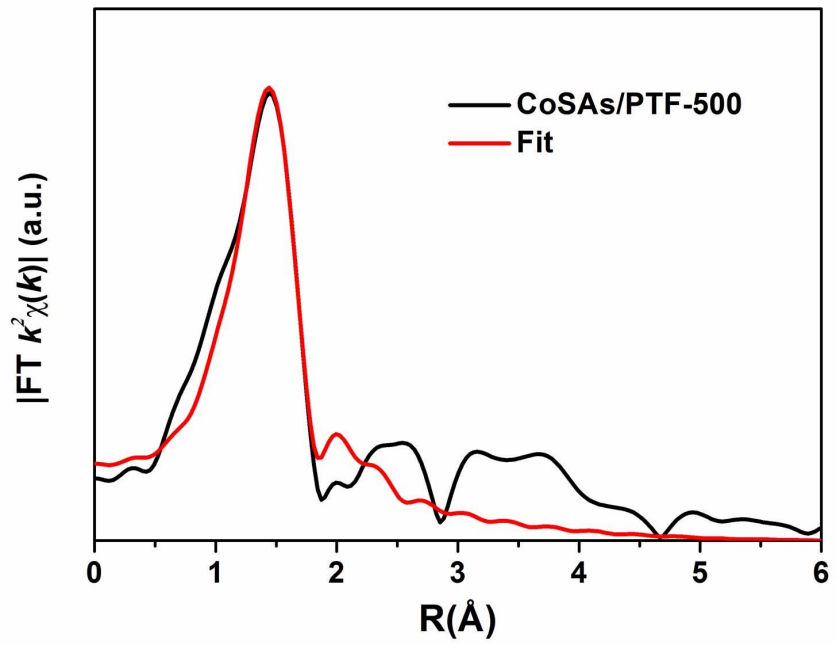

Figre S12. EXAFS fitting curves of CoSAs/PTF-500.

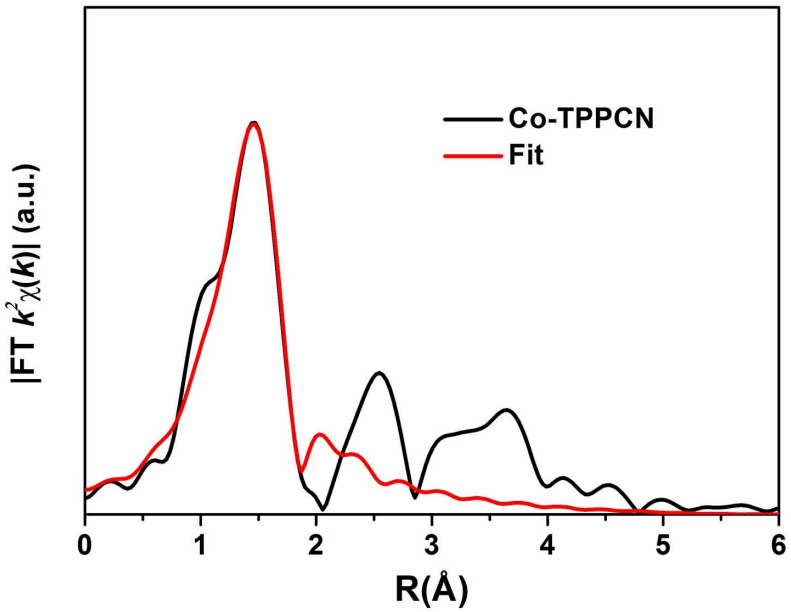

Figre S13. EXAFS fitting curves of Co-TPPCN.

Table S6 Comparison of ORR catalytic performances in alkaline solution between CoSAs/PTF-600 and other noble-metal-free electrocatalysts reported previously.

Catalyst	Onset potential (V)	$E_{1/2}$ (V)	Current density (mA/cm^2) at 0.2 V	Refs.
CoSAs/PTF-600	0.92	0.81	6.14	This work
MOFCN	0.92	0.72	4.10	S1
GPC-1000-5	0.87	0.71	5.40	S2
FeIM/ZIF-8	0.91	0.76	5.00	S3
Co@Co_3O_4@ C-CM	0.93	0.81	4.60	S4
Fe−N/C-800	0.92	0.81	6.06	S5
OMC	0.81	0.69	3.10	S6
HPC-N-850	0.90	0.78	4.20	S7
Fe-N/G	0.87	0.78	5.21	S8
N:C-MgNTA	0.89	0.75	5.70	S9

*Note: all potentials are versus to reversible hydrogen electrode (RHE).

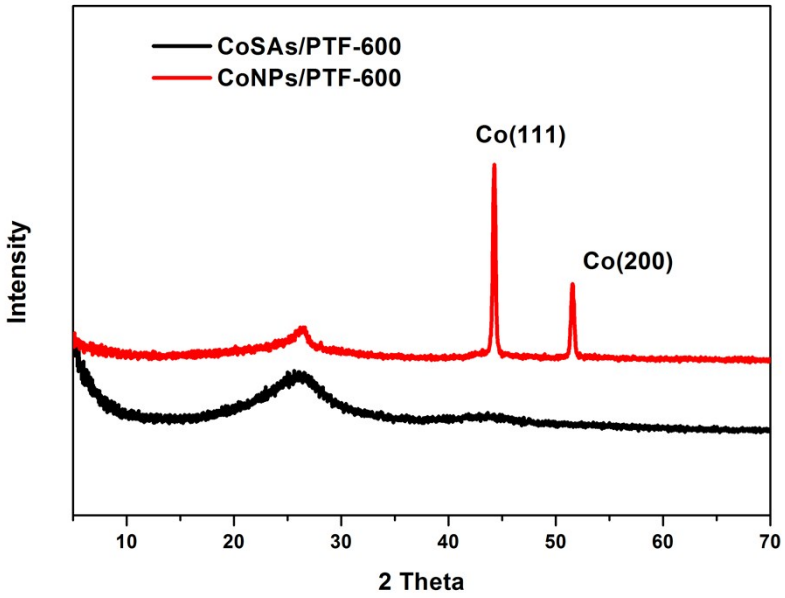

Figure S14. PXRD patterns of CoSAs/PTF-600 and CoNPs/PTF-600.

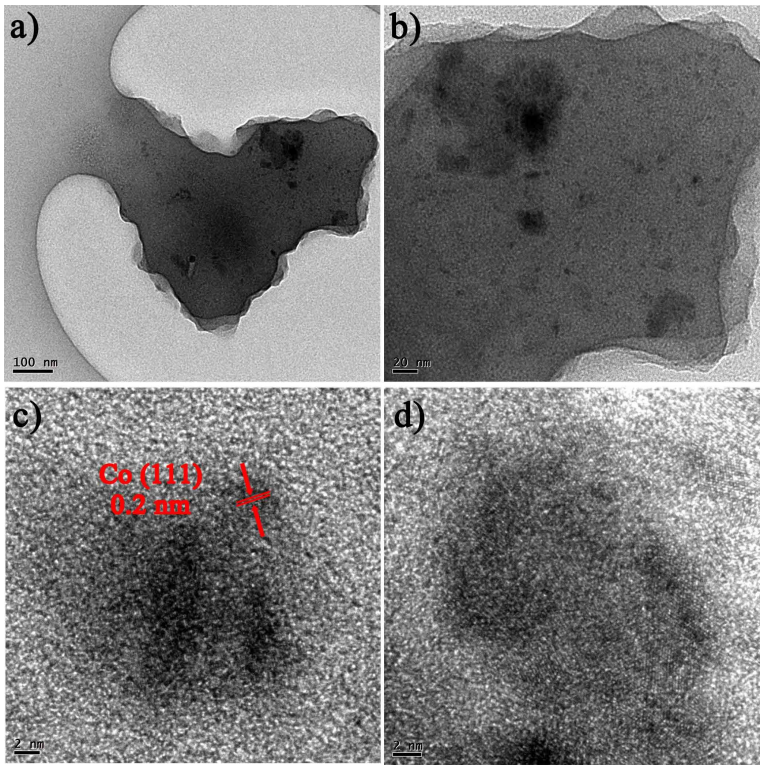

Figure S15. TEM and HRTEM images of CoNPs/CTF-600.

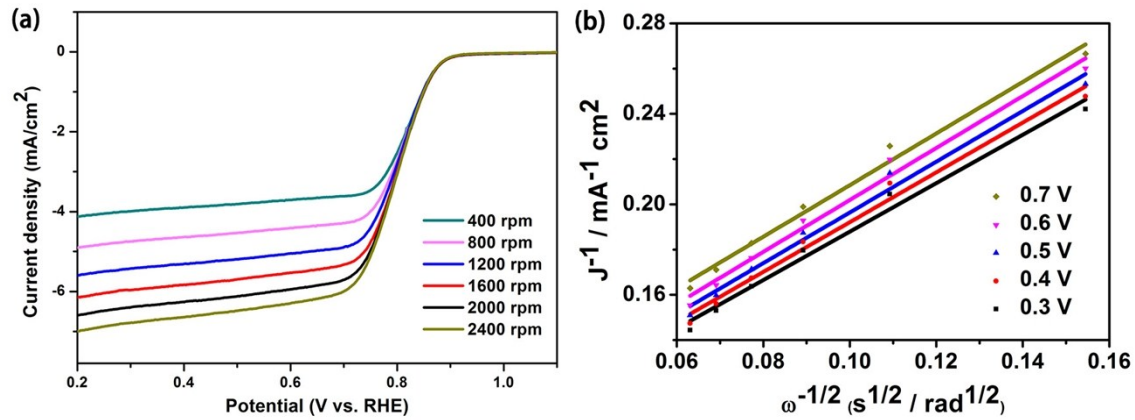

Figure S16. (a) LSV of CoSAs/PTF-600 at different rotation speeds. (b) K-L plots.

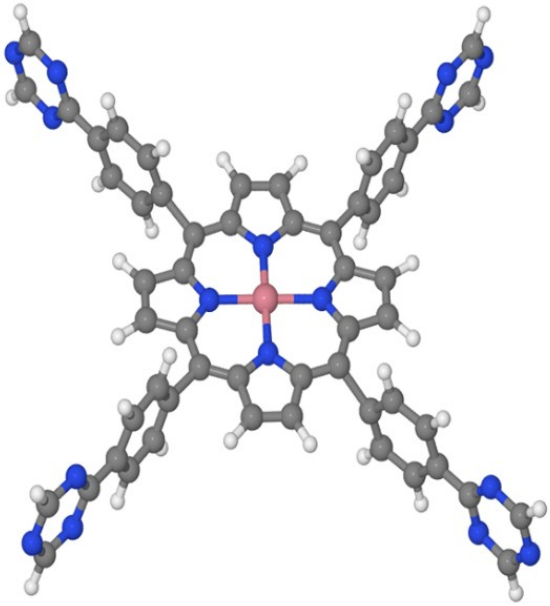

Figure S17. The atomic structure of CoSAs/PTF. The pink, white, grey and blue spheres denotes Co, H, C and N atoms, respectively.

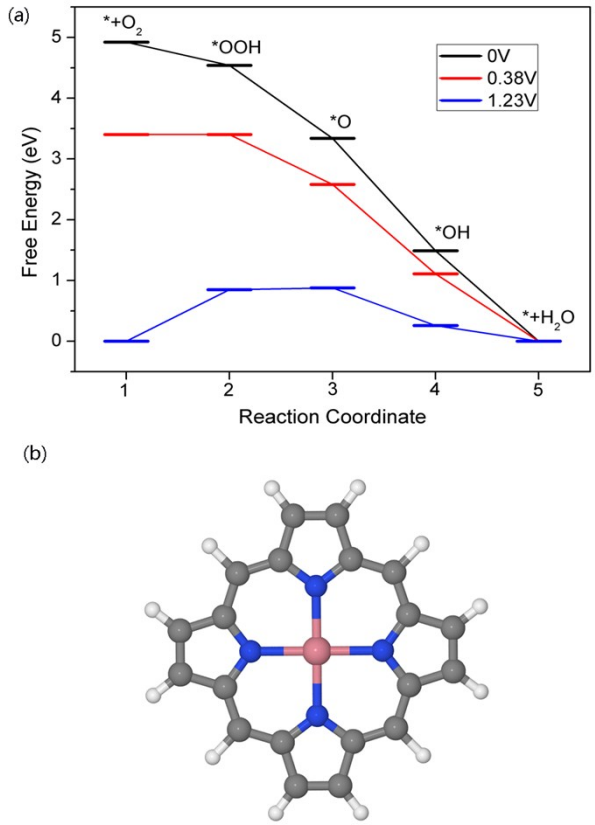

Figure S18 (a) The free energy variations for Co-porphyrin during the ORR process. The black, red and blue lines are for ORR under electrochemical potentials of 0, 0.38 and 1.23 V, respectively. (b) The atomic structure of Co-porphyrin. The pink, white, grey and blue spheres denotes Co, H, C and N atoms, respectively.

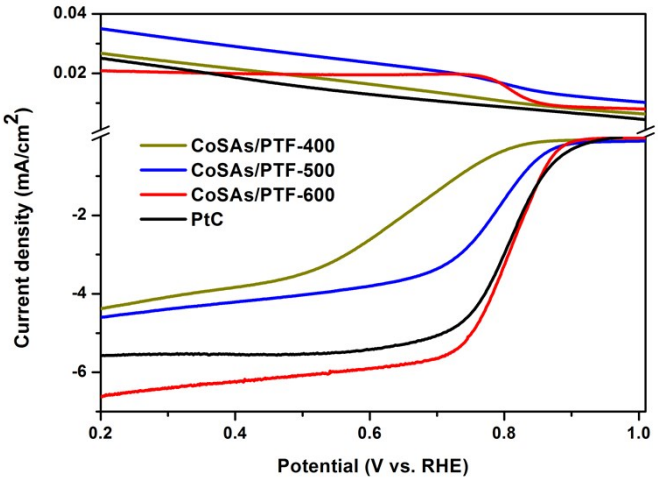

Figure S19. The LSV cures of rotating ring-disk electrode (RRDE) measurements of Pt/C and CoSAs/PTF-400, 500, 600.

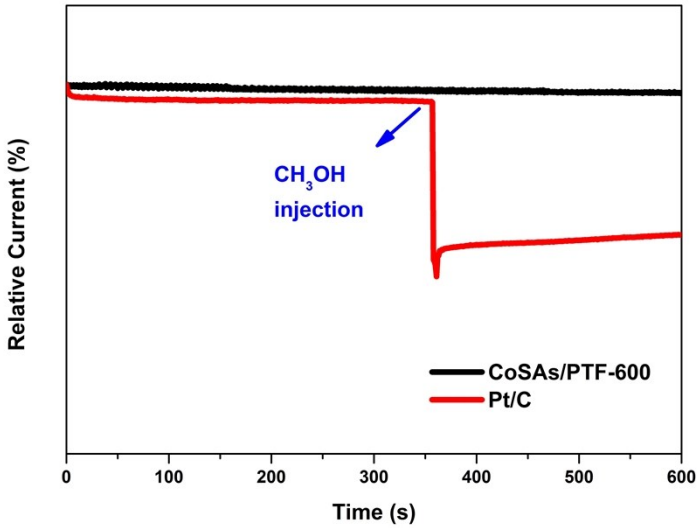

Figure S20. Methanol-crossover effects test of CoSAs/PTF-600 and Pt/C.

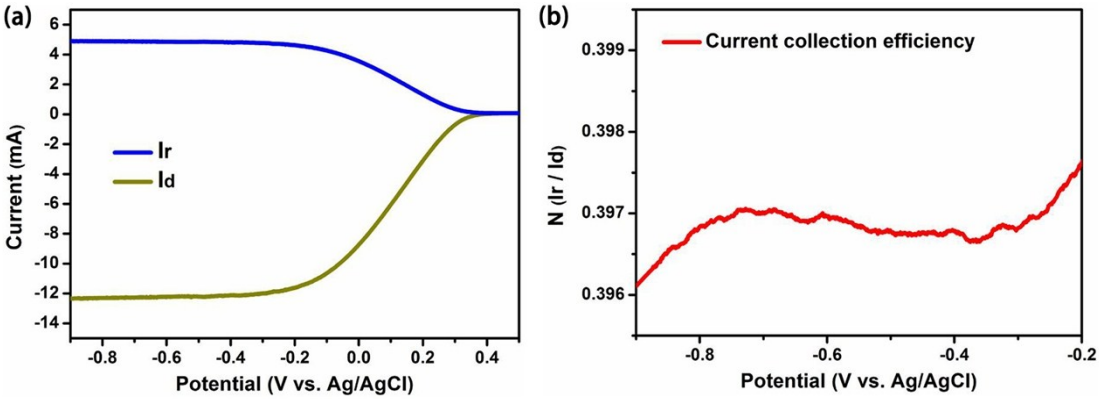

Figure S21. Measuring the current collection efficiency N of RRDE in N_2-saturated 0.1 M $K_3[Fe(CN)_6]$ solution with a constant ring potential of 0.5 V vs. Ag/AgCl. (a) LSV of RRDE with a scan rate of 10 mV/s (Id is disk current, Ir is ring current). (b) The current collection efficiency N is calculated with the following equation: N = Ir / Id.

References.

1. S. Pandiaraj, H. B. Aiyappa, R. Banerjee, S. Kurungot. *Chem. Commun.* **2014**, 50, 3363-3366.
2. L. J. Zhang, Z. X. Su, F. L. Jiang, L. L. Yang, J. J. Qian, Y. F. Zhou, W. M. Li, M. C. Hong, *Nanoscale* **2014**, 6, 6590-6602.
3. D. Zhao, J. L. Shui, C. Chen, X. Chen, B. M. Reprogle, D. Wang, D. J. Liu, *Chem. Sci.* **2012**, 3, 3200.
4. W. Xia, R. Zou, L. An, D. Xia, S. Guo, *Energy Environ. Sci.* **2015**, 8, 568.
5. L. Lin, Q. Zhu and A. Xu, *J. Am. Chem. Soc.* **2014**, 136, 11027-11033.
6. S. Lee, M. Choun, Y. J. Ye, J. Lee, Y. Mun, E. Kang, J. Hwang, Y. Lee, C. Shin, S. Moon, S. Kim, E. Lee, J. Lee, *Angew. Chem. Int. Ed.* **2015**, 54,9230.
7. G. J. Tao, L. X. Zhang, L. S. Chen, X. Z. Cui, Z. L. Hua, M. Wang, J. C. Wang, Y. Chen, J. L. Shi, *Carbon* **2015**, 86,108.
8. Q. Lai and Q. Su, *ACS Appl. Mater. Inter.* **2015**, 7, 18170–18178.
9. D. Eisenberg, W. Stroek, N. J. Geels, C. S. Sandu, A. Heller, N. Yan, G. Rothenberg, *Chem. Eur. J.* **2016**, 22, 501-505.